CSI-independent Non-linear Signal Detection in Molecular Communications

Bin Li, *Member, IEEE*, Weisi Guo, *Senior Member, IEEE*, Xiang Wang, Yansha Deng, *Member, IEEE*
Yueheng Lan, Chenglin Zhao, A. Nallanathan, *Fellow, IEEE*

***Abstract*—Molecular communications rely on diffusive propagation to transport information, which is attractive for a variety of nano-scale applications. Due to the long-tail channel response, spatial-temporal coding of information may lead to severe inter-symbol interference (ISI). Classical linear signal processing in wireless communications is usually operating with high complexity and high signal-to-noise ratios, whereas signal processing in molecular communication system requires operating in opposite conditions. In this work, we propose a novel signal processing paradigm inspired by the biological principle, which enables low-complexity signal detection in extremely noisy environments. We first propose a non-linear filter inspired by stochastic resonance, which is found in a variety of biological systems, and it can significantly improve the output SNR by converting noise to useful signals. Then, we design a non-coherent detection method, one which exploits the generally transient trend of observed signals (i.e. quick-rising and slow-decaying) rather than hidden channel state information (CSI), thus excluding CSI estimation and involving only summations. Implementation issues are also discussed, including parameters configuration and adaptive threshold. Numerical results show that the proposed bio-inspired scheme can improve the performance remarkably over classical approaches. Even compared with the optimal linear methods, the required SNR of the proposed scheme can be reduced by 7dB, which reaffirms why it can be used in noisy biological environments. As the first attempt to design bio-inspired molecular signal detectors, the proposed non-linear processing paradigm may provide the great promise to the emerging nano-machine applications.**

***Index Terms*—Molecular communications, CSI-independent, non-linear signal processing, stochastic resonance, transient feature, non-coherent detector**

I. Introduction

MOLECULAR communication is the foundation of cell-to-cell interaction in multi-cellular organisms [2]–[4]. In recent years, inspired by a variety of biological communication systems (e.g. pheromone signaling [1]), telecommunication engineers have been developing bio-inspired systems to enable robust information transfer in various adverse environments [2], [6], [9], [11]. These molecular communication systems are in direct contrast to man-made (or artificial) telecommunication system, which relies on complex signal processing and information modulation on electromagnetic waves (EMW) [5]. As such, molecular communications constitute a new framework of information transportation, which is more effective in harsh biological environments where EMW signaling cannot propagate efficiently through complex structures or fluid mediums. By replacing EMW carrier with a set of chemical molecules, the information transmission can be realised with low energy levels. Furthermore, low-complexity electronic implementation is possible through the development of new family of signal processing techniques [7], [8]. Together these make molecular communications an enabling technique to future nano-medicine or nano-surgery applications [9], [10].

The first prototype systems capable of generalised information encoding was developed in [6]. Thereafter, initial approaches to develop robust signal processing techniques have focused on evolving classical EMW-based signal detection schemes [13]–[15]. In [13], coherent detection techniques, such as maximum *a posteriori* (MAP) detector and maximum likelihood (ML) scheme, are applied to combat the diffusion propagation by fully utilising channel state information (CSI) [15]. Such linear detectors, (i.e. relying on summation and multiplication), would achieve the promising (or even optimal) performance [14]. As far as emerging applications (i.e. nano-machine communications) are concerned, however, the aforementioned methods may become less attractive.

On one hand, acquiring unknown CSI of diffusive channel is usually resource demanding, in terms of both time and energy. Various techniques, such as machine learning, have been suggested, all of which involve a large computational burden and potentially a large number of training data sets. On the other hand, in order to mitigate serious inter-symbol interference (ISI) aroused by a long-tail diffusive channel response, the computational complexity tends to be unaffordable [16]. Thus, the low-complexity detector becomes a promising alterative. For example, in [17] the energy detection is developed. In [18], as one special case of optimal coherent ML detector, a fixed-threshold based non-coherent detector is designed, which obtains the promising performance in the case of negligible ISI (e.g. low data-rate). For many realistic applications with serious ISI, such a fixed-threshold detector may become invalid. Last but not least, the above linear processing techniques usually require high signal-to-noise

Bin Li and Chenglin Zhao are with the School of Information and Communication Engineering (SICE), Beijing University of Posts and Telecommunications (BUPT), Beijing, 100876, China. (Email: stonebupt@gmail.com).

Xiang Wang is with Beijing Jianyi Corporation Limited Company, Beijing, China. (Email: wangxiang@jianea.com)

Weisi Guo is with School of Engineering, University of Warwick, West Midlands, CV47AL. (Email: Weisi.Guo@warwick.ac.uk)

Yansha Deng is with Department of Informatics, King's College London, London, United Kingdom. (Email: yansha.deng@kcl.ac.uk).

Yueheng Lan is with the School of Sciences, Beijing University of Posts and Telecommunications (BUPT), Beijing, 100876, China. (Email: lanyh@bupt.edu.cn).

A. Nallanathan is with the School of Electronic Engineering and Computer Sciences, Queen Mary-University of London, London, United Kingdom. (Email: nallanathan@ieee.org)

Manuscript received January 17, 2018.

ratios (SNR) to achieve the desired performance. This tends to be the greatest obstacle when applying existing schemes to molecular communications which operates in noisy and disturbing biological environments.

Over the past two decades, there is growing recognition that the answer to robust noisy signal detection may lie in naturally biological mechanisms [19], [20], which remain quite different from the aforementioned *artificial* signal processing techniques. For example, the biologically dynamical process could amplify cell signaling in noisy environments, by creating a stochastic resonance (SR) effect. This attractive SR mechanism is characterized by a bi-stable nonlinear dynamical system, whereby the noisy signal serves as an input force. After altering the potential function of this nonlinear dynamical system, the output transits between two stable states synchronous to a weak bias (i.e. input signal), with the aid of noise. Thus, the output SNR is significantly enhanced.

Inspired by this, we propose a novel CSI-independent non-linear signal processing scheme for molecular communications, whereby we leverage non-linear biological principles and design a simple yet effective detection algorithm. Our nonlinear detector uses the SR technique to improve detection SNRs (i.e. involving nonlinear operation, not only addition and multiplication), and exploits the transient features of filtered waveform to detect signals. Note that, the resulting non-coherent detector, which was firstly proposed in [7], [16], excludes the CSI estimation and the complex equalization, thereby more attractive to molecular communications. To sum up, our contributions are summarised as follows.

1. We propose a non-linear signal filter to improve the detection SNR by constructively exploiting random noise. In contrast to a linear filter, our emphasis is not just to filter out noise, but also tune it into useful component of output signals. When the SR mechanism is established, the output response becomes a noise-reduced while signal-enhanced version of the input force, and the output SNR will be improved.

2. We develop a CSI-independent and non-coherent signal detector. Rather than focusing on CSI acquisition and channel equalisation, we resort to certain inherently transient features of filtered waveforms. Three independent metrics are thereby constructed. Distinguished from previous non-coherent schemes which only exploits the partial feature (e.g. local convexity [16]) and is vulnerable to noise, we designed a robust CSI-independent framework by completely utilizing the whole transient features of received signal. Except for the exclusion of CSI, our compound metric even provides diversity gain, as these sub-metrics reflect the same information whilst involving independent noise.

3. We discuss the implementation issues of our proposed non-linear non-coherent signal detector. Different from the conference version [22], detailed structures of both non-linear filter and non-coherent detector are studied. For a non-linear filtering process, the practical parameter configurations of potential function are investigated, in both cases of known and unknown noise variance. For a CSI-independent detector, a blindly adaptive threshold scheme is designed to derive final decision from the constructed metric, which is shown to be effective even when CSI remains unknown.

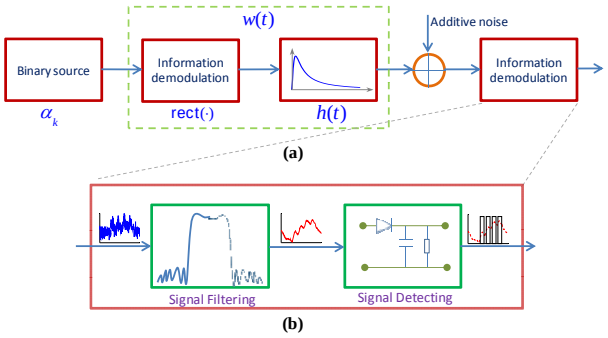

Fig. 1. (a) A shared schematic structure of both EMW-based communications and molecular communications. (b) In the stage of information demodulation, usually the signal filtering (e.g. band-pass filter) and signal detecting (e.g. envelop detection) will be implemented.

4. We evaluate the detection performance of our proposed method. Various effects in implementation are studied via numerical simulations, including algorithm parameters and transmission configurations. It is shown that the output SNR after a non-linear filter will be enhanced, by constructively utilising random noise (rather than treating it as a destructive component as usual). Furthermore, with the CSI independent signal detector, the performance can be significantly improved even when comparing with that of optimal coherent detector. Our non-linear non-coherent detector constitutes a novel model-free signal processing paradigm, which is inspired by long-standing biological concepts that are distinguished from those known techniques in EMW-based communications. It will be not only of great promise to molecular communications in harsh biological environments, but potentially open a new perspective for EMW-based communications.

The rest of this article is structured as follows. In Section II, a general system model is established, and existing coherent detectors are briefly introduced. In Section III, a non-linear filtering scheme relying on SR is studied, including its principles, configurations and implementations. Then, the non-coherent detection scheme is designed in Section IV. In Section V, numerical simulations are provided to validate our scheme. We finally conclude this study in Section VI.

The notations used in this work are summarized as follows. The $n \times 1$ dimensional vector is denoted by $\mathbf{x}_{n\times 1}$, and the $M \times N$ matrix is $\mathbf{X}_{M\times N}$; $|x|$ is the absolute value of variable x, and $\langle x \rangle$ gives the conditional and ensemble averaging over noises; $\partial f(x;t)/\partial x$ gives the partial derivative of $f(x;t)$ on x, while $\partial^2 f(x;t)/\partial x^2$ gives the second-order partial derivative, and $\nabla f(x,y,z;t)$ is the Laplace operator in cartesian coordinates; $(\cdot)^T$ denotes the transpose; $\otimes$ denotes the convolution operation; $diag(\cdot)$ gives a block matrix having the arguments along its main diagonal; $\mathcal{A}$ denotes one specific set; $\mathbb{E}(\cdot)$ is the ensemble average.

II. SYSTEM MODELS

A. Molecular Communications

A generalized model for the MC system is shown in Fig. 1-(a) [23], [24], which involves three following components.

*1) **Information source**:* An information source may be either a single cell/organism in a biological system, or a simple hardware transmitter in man-made system. Rather than EMW carriers, it emits a certain amount of chemical molecules to carry the information. The information will be encoded (or modulated) by amplitude (i.e. concentration) or phase (i.e. interval), as in biological systems. Taking the amplitude modulation (AM) for example [4], [25], in each symbol duration T_b a transmitter will release a short impulse molecules with a duration T_p, which contains a total of Q molecules at time k if the binary symbol $\alpha_k \in \mathcal{A} = \{0, 1\}$ is 1 ($k = 0, 1, \cdots, \infty$). Otherwise, in the case of $\alpha_k = 0$, there is no molecule released, i.e.,

$$s(t) = Q \cdot \sum_{k=0}^{\infty} \alpha_k \times \texttt{rect}\left(\frac{t - T_p/2}{T_p} - kT_b\right). \quad (1)$$

Here, a rectangular pulse shaper $\texttt{rect}(\cdot)$ is adopted. In a biological system, the binary information symbol may lead to quite different cell responses, e.g. "1" for cell proliferation and "0" for cell death [3].

*2) **Propagation channel**:* In contrast to EMW-based communications, a propagation channel for molecular messengers is characterized by random diffusion [26]. Taking the 1-D free diffusion for example, according to the Fick's second law [27], the decay of molecular concentration (or channel gain) is proportional to its flux, i.e.

$$\frac{1}{C} \cdot \frac{\partial p(x;t)}{\partial t} = \nabla p(x, y, z; t), \quad (2)$$

where

$$\nabla p(x, y, z; t) \triangleq \frac{\partial^2 p(x, y, z; t)}{\partial x^2} + \frac{\partial^2 p(x, y, z; t)}{\partial y^2} + \frac{\partial^2 p(x, y, z; t)}{\partial z^2},$$

and C is the constant diffusion coefficient, which is specified by the Einstein relation, i.e. $C = \frac{\kappa_B T}{6\pi\gamma R_m}$. Here, $\kappa_B = 1.38 \times 10^{-23}$J/K is the Boltzmann constant [26]; T is the temperature in Kelvin; γ is the viscosity of the propagation media; R_m is the radius of molecular particle.

Subjected to the initial condition $p(x, y, z; 0) = \delta(x)\delta(y)\delta(z)$, the analytical solution of above partial differential equation (PDE), which accounts for the expected concentration for a given travelling time $t > 0$ and a transmitter-receiver distance d, reads [28], [30]:

$$\bar{h}(t; d) = \frac{1}{(4\pi C t)^{3/2}} \times \exp[-d^2/(4tC)]. \quad (3)$$

Note that, here the Passive receiver with an expected channel response $\bar{h}(t; d)$ is considered, which is used to establish a common system model for other counterpart methods (e.g. MAP and MMSE). As we will see later, our developed non-coherent detector should be independent of any specific receptor and channel response, owning to its CSI-independent nature. So, it is readily applicable to other types of receiver with various CSI, e.g. the absorbing receiver [32], [33], the passive receiver with enzymes [35], the absorbing receiver with enzymes [34] and ligand receptor with binding effect [36]. In this study, rather than the property of different receivers, we are specially interested in the design of robust non-coherent detector that could be generalised to various CSI.

*3) **Information sink**:* The sink is a receptor of information-modulated molecular messenger. As in EMW-based wireless communication systems, the additive noise is considered, and the received signal is modeled as:

$$y(t) = s(t) \otimes w(t) + z(t). \quad (4)$$

Here, we consider a linear system model [13], and the notation $\otimes$ denotes the convolution [31]; $w(t) = \texttt{rect}[(t - T_p/2)/T_p - kT_s] \otimes h(t)$ (for clarity, the other variable d is omitted here) gives the equivalent channel between the binary information source $\{\alpha_k\}$ and a nano-receiver, as in Fig. 1-(a). $z(t)$ denotes the additive noise term.

B. Equivalent Signal Model

At receiver, a detector firstly samples the molecular concentration with the Nyquist rate $R = 1/T_s = 1/T_b$ [31], i.e. $T_s = T_b$. After doing so, the discrete signal is written as

$$y_k = \sum\nolimits_{l=0}^{\infty} \alpha_l \times w_{k-l} + z_k, \quad (5)$$

where $y_k = y(kT_b)$, $w_k = w(kT_b - lT_b)$ and $z_k = z(kT_b)$. For a causal system, we have $w_{k-l} = 0$ if $k - l < 0$. Without the loss of generality, the synchronization has been accomplished accurately [29], and we further have:

$$y_k = \alpha_k w_k + \sum_{l=k-1}^{I} \alpha_l w_{k-1-l} + z_k. \quad (6)$$

Owing to the long-tail diffusion channel response, serious ISI is inevitable. As in Eq. (6), I is referred to as the memory length, which specifies the ISI length from previous intervals. When the passive receiver is used, I may tend to be an unbounded value. For the other cases, a finite value may be assumed. In the following analysis, a truncated memory length is considered.

*1) **Signal-dependent noise**:* As one important feature in the MC system, the additive noise would become dependent of the received signal, owing to the imperfect sampling/counting process at the receptor [13], [21], [33], [37] (or more simply, the random Brownian movement of molecular messengers [38]). That means, the noise variance is no longer a constant as in EMW-based wireless communication systems, but keeps proportional to the expected concentration at the current time index k. Accordingly, we adopt the following signal-dependent noise model, i.e.,

$$y_k = \text{Poisson}\,(s_k) + \mathcal{N}(0, \eta s_k), \quad s_k \triangleq \sum\nolimits_{l=0}^{\infty} \alpha_l \bar{w}_{k-l}, \quad (7)$$

where s_k is the expected time-dependent concentration; η is the scaled parameter related with the diffusion coefficient C and the the radius of the receptor space [21].

Note that, the binomial distribution is originally used in modeling the received noise. I.e., N_R interfering molecular particles may arrive at the receptor independently with an equal probability p_R. For the ease of analysis, this statistical distribution can be approximated by a Poisson distribution [21], [38] (e.g. N_R is large and p_R is small) or a Gaussian distribution [13], [22] (e.g. $N_R p_R$ is relatively large).

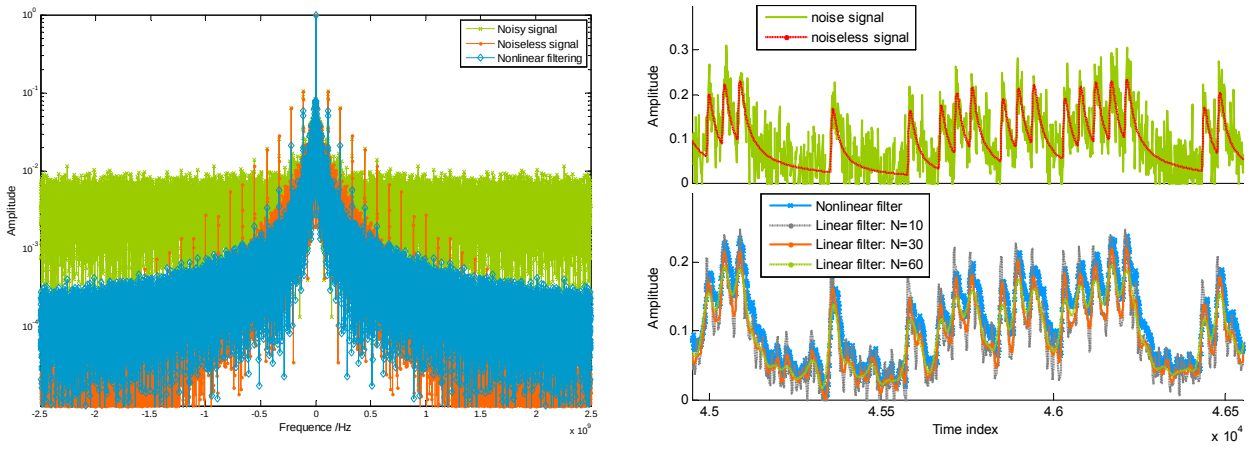

(a) (b)

Fig. 2. (a) The power spectrum of received noisy signals $y(t)$, as well as the output signal $x(t)$ after the non-linear filtering. Note that, the power spectrum has been normalized by the maximum value. The SNR is configured to 5dB. (b) *Top*: Time waveform of the received noisy signal and noiseless signals. *Bottom*: The output of both linear and non-linear filter considered by this work. Here, a window-based finite impulse response (FIR) filter is studied. A Kaise window is used and the ripple of passing band 0.01. Three FIR filter orders are considered, i.e. $N = 10$, $N = 60$ and $N = 70$.

*2) **Signal-independent noise**:* Despite the theoretic significance of signal-related noise in MC systems, it may arouse additional difficulties. Except for the complex CSI estimation, the well-designed adaption mechanism should be integrated to deal with this non-stationary noise. More importantly, it would be infeasible to exactly know the time-varying noise variance (as the received signal itself is uncertain before detection).

In contrast, our non-coherent detector requires the little information on CSI and noise, by focusing on the slow-changing transient shape of received signal (corrupted by the additive noise). So, it could be applicable to both signal-dependent and signal-independent noises. In fact, the signal-independent noise would permit the designing of more robust non-coherent signal detector. With the simplified signal-independent noise (with a variance σ_z^2), the received signal is reformulated as:

$$y_k = \text{Poisson}\left(s_k\right) + \mathscr{N}(0, \sigma_z^2).$$

C. Linearly Coherent Detection

*1) **MAP detector**:* For convenience, a vector expression of received signal is formatted as $\mathbf{y} = \mathbf{W}\boldsymbol{\alpha} + \mathbf{z}$, where $\mathbf{y} = [y_0, y_1, \cdots, y_K]^T$; $\mathbf{W}$ denotes a circulant channel matrix constructed from $\mathbf{w}$, while $\mathbf{z}$ is the noise vector. In general, the MAP detector aims to maximize the posterior probability density function (PDF) of unknown information symbols conditioned on received samples, i.e.,

$$\begin{aligned}\hat{\boldsymbol{\alpha}}_{\text{MAP}} &= \arg\max_{\boldsymbol{\alpha}\in\mathcal{A}^K} P(\boldsymbol{\alpha}|\mathbf{y}, \mathbf{W}),\\ &= \arg\max_{\boldsymbol{\alpha}\in\mathcal{A}^K} \prod_{k=0}^{K} p(\alpha_k|\alpha_{0:k-1}) \cdot \prod_{k=0}^{K} p(y_k|y_{0:k-1}, \alpha_{0:k}). \quad (8)\end{aligned}$$

Given the i.i.d Gaussian noise, the likelihood densities $p(y_k|y_{0:k-1}, \alpha_{0:k})$ will follow the normal distribution [13]. It is noteworthy that, in the above coherent MAP, the accurate estimation of CSI [12] will be indispensable in evaluating the likelihood function or mitigating the ISI [15]. As seen, the complexity of such an MAP scheme comes from the sequential computation of likelihoods [16]. When a binary information source with the equal prior probability is considered, the MAP scheme tends to be an ML detector.

*2) **MMSE detector**:* Another popular linear detector is inspired by the MMSE criterion [31], which aims to minimize the covariance matrix of detection errors, i.e.,

$$\hat{\boldsymbol{\alpha}}_{\text{MMSE}} = \arg\max_{\boldsymbol{\alpha}\in\mathcal{A}^K} \mathbb{E}\left[(\boldsymbol{\alpha} - \hat{\boldsymbol{\alpha}})(\boldsymbol{\alpha} - \hat{\boldsymbol{\alpha}})^T\right]. \quad (9)$$

Based on the linearly Gaussian model as in eq. (4), the MMSE estimation is derived via:

$$\begin{aligned}\hat{\boldsymbol{\alpha}}_{\text{MMSE}} &= \mathbb{E}(\boldsymbol{\alpha}|\mathbf{r}),\\ &= \mathbb{E}(\boldsymbol{\alpha}) + \boldsymbol{\Gamma}_z\mathbf{W}^T(\mathbf{W}\boldsymbol{\Gamma}_z\mathbf{W}^T + \boldsymbol{\Gamma}_z)^{-1}(\mathbf{y} - \mathbf{W}\boldsymbol{\alpha}), \quad (10)\end{aligned}$$

where $\mathbb{E}(\cdot)$ represents the ensemble average; $\boldsymbol{\Gamma}_z = diag\{[\sigma_z^2, \cdots, \sigma_z^2]\}$ is the $K \times K$ diagonal matrix with its elements are all σ_z^2. In the above MMSE scheme, the accurate CSI will be also indispensable.

D. Nonlinear DFE Detector

Different from a linear MAP detector, a decision-feedback equalizer (DFE) belongs to the sub-optimal and nonlinear detector, which is composed of a feed-forward filter and a feedback filter [13], [18]. Denote the coefficient vectors of feed-forward and feedback components with $\mathbf{f}_q \in \mathbb{R}^{L\times 1}$ and $\mathbf{g}_q \in \mathbb{R}^{B\times 1}$ (L and B respectively denote the tap length of feed-forward and feedback filters), then the detected symbol of time k is:

$$\hat{\alpha}_k = \sum_{q=0}^{L-1} f_q z_{k-q} + \sum_{q=1}^{B} g_q \hat{\alpha}_{k-q-1}. \quad (11)$$

Unlike both MAP and MMSE detectors, the DFE method estimates the optimal coefficients vector $\mathbf{f}_q$ and $\mathbf{g}_q$ without explicitly knowing the channel response $w(t)$. To do so, it exploits a group of training symbols $\boldsymbol{\alpha}'_k$ (which consumes additional time and energy resource) to update the filter

coefficients [40], e.g. via the normalized least-mean-square (Norm-LMS) algorithm,

$$\mathbf{f}_q(k) = \mathbf{f}_q(k-1) + \mu/||\mathbf{m}_f(k)||_2^2 \cdot e(k)\mathbf{m}_f(k), \quad (12)$$

$$\mathbf{g}_q(k) = \mathbf{g}_q(k-1) + \mu/||\mathbf{m}_g(k)||_2^2 \cdot e(k)\mathbf{m}_g(k), \quad (13)$$

where $\mathbf{m}_f(k)$ and $\mathbf{m}_g(k)$ denote the received signal vector and the decision bits vector in a feedback filter, respectively; $e(k) = \boldsymbol{\alpha}_k' - \mathbf{m}_g(k)$ is the error and $\mu \in (0,1)$ is the step size.

III. NONLINEAR FILTERING

A. Non-linear vs Linear Filtering

In order to suppress background noise, a filtering process will be necessary. When the useful frequencies are known as *a priori*, the well-studied linear filter, e.g. finite impulse response (FIR) filter, can be applicable, which filters out the high-frequency noise and passes only the low-frequency useful signal. As noted, there is a compromise in the designing of linear filter, whereby the temporal sharp transitions will be smoothed at the same time of suppressing high-frequency noise, as shown in Fig 2. (b), which may degrade detection performance to some extent. More importantly, such linear schemes may incur the high complexity to implementation (e.g. requiring dozens of delayed taps and multipliers).

Inspired by the biological and physical concepts, a non-linear filter scheme, in contrast, may be premised on specific stochastic PDE (SPDE), which has the great potential of suppressing useless noise whilst enhancing useful signal. We focus on such a nonlinear dynamical mechanism and the filtered signal was demonstrated in Fig 2. (b), where the subtle features of molecular signaling are preserved at the same time of mitigating useless noise. From this perspective, a non-linear filter will be of great promise to molecular communications, whereby the biological noise (aroused by random disturbances and variations of bio-activities) is extremely strong, whilst signal distortions may lead to disastrous consequences.

In the following, we will exploit the non-linear SR to process the received noisy signal. First, we simply show the underlying physical principles. Then, we discuss the related implementation issues of our non-linear filter.

B. Stochastic Resonance

The SR concept was originally proposed when studying the periodically recurrent ice ages [41], [42]. It provides an intriguing statistical explanation on the average periodicity around 10^5 year, which is a direct result modulated by a weak force, i.e., the period of earth's orbital eccentricity. Despite weak effects of the external force, the output response would be amplified by internal noise. With the periodical bias from external force and the aid of noise, the outcome states would hop coherently among two-stable states (i.e. cold and warm) [43], [44]. Inspired by this, a new scheme to deal with noise was established. Surprisingly, an extra dose of noise could help rather than hinder the performance improvement.

1) Basic Principle: Consider the bi-stable dynamical system characterized by a double-well potential function $V(x)$:

$$V(x) = -a/2 \cdot x^2 + b/4 \cdot x^4, \quad (14)$$

which has two minima located at $x_m = \pm\sqrt{a/b}$, corresponding to two stable states, see Fig. 3-(a). The potential barrier, with a height of $\Delta V = a^2/4b$, is located in the middle of two stable states, and an unstable local maximum at x_b=0.

Just imagine if one heavily-damped particle (e.g. with a mass m and the viscous friction γ) is put in this double-well potential $V(x)$, it would randomly jump across the potential barrier and transit to another stable state, subject to internal noise forcing. The transitional rate, as a reciprocal of mean first passage time (MFPT), is given by the Kramers rate [44]:

$$r_0 = \frac{\varpi_0 \varpi_b}{2\pi\gamma} \times \exp\left(-\frac{\Delta V}{D}\right). \quad (15)$$

where D denotes the variance of internal noise. Two squared angular frequencies ϖ_0 and ϖ_b, evaluated respectively at the minima x_m and the barrier x_b, are given by:

$$\varpi_0 = \left|d^2V(x)/dx^2\big|_{x=x_m}\right| = 2a,$$
$$\varpi_b = \left|d^2V(x)/dx^2\big|_{x=x_b}\right| = a. \quad (16)$$

If further superimposing a weak periodic force, e.g. $A_0 \times \cos(\Omega t + \varphi)$, onto the above stochastic dynamical system, then the motion of the Brownian particle will be governed by the Langevin equation. For a large friction coefficient γ, the underlying dynamical system reads:

$$\gamma\frac{dx(t)}{dt} = -\frac{1}{m}\frac{dV(x)}{dx} + A_0 \cdot \cos(\Omega t + \varphi) + \sqrt{2\gamma D}\xi(t). \quad (17)$$

where Ω and φ denote the frequency and phase of external periodic force; $\xi(t)$ accounts for internal random fluctuation, which is modeled by white Gaussian noise[1], with an auto-correlation function $\langle\xi(t+\tau)\xi(t)\rangle = \delta(\tau)$, where $\delta(\cdot)$ is the Dirichlet-function.

It is seen that the output $x(t)$ is closely related with a double-well potential $V(x)$. A simple illustration of the dynamical system behavior is given by Fig. 3. The periodical external force alters the potential barrier $\Delta V_{\pm}$, rendering the state transition from one side to the other much easier. With the suitable dose of noise, the system outcomes may transit coherently among two stable states. Once the synchronized rhythm between the noise-induced transition and the periodic input is accomplished, the outcome is significantly enhanced, by transforming part of noise to the output signal. To establish this SR, the average waiting time $T_0(D) = 1/r_0$ between two noise-induced transitions should be equivalent to a half of the input periodicity $T_\Omega = 2\pi/\Omega$, i.e.,

$$T_0(D) = \frac{1}{2}T_\Omega = \frac{\pi}{\Omega}. \quad (18)$$

[1]For the simplicity of analysis, the signal-independent Gaussian noise with a constant variance is widely used [44], [45]. It is noted that, however, any additive noise can be utilized to enhance the system output, regardless of the noise distribution or the time-dependence of noise variance. For the non-stationary noise, yet the optimal operation of the nonlinear SR would require the adaption of parameters, according to the time-dependent noise characteristics.

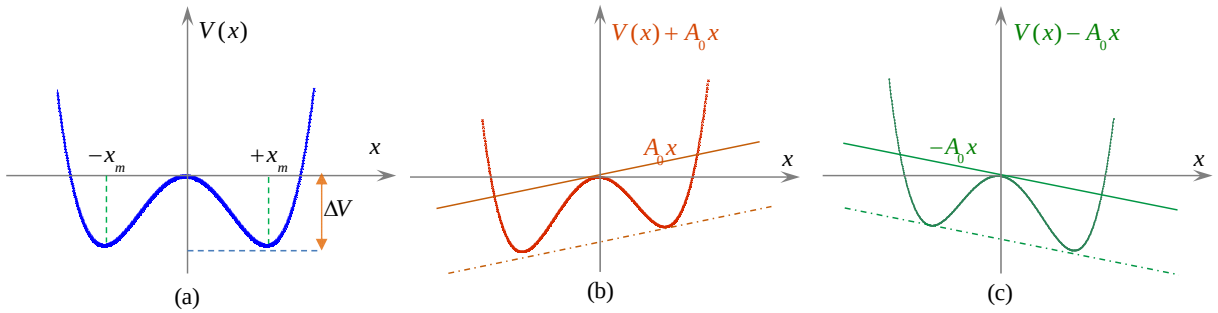

Fig. 3. (a) The double-well potential of the non-linear dynamical system, i.e., $V(x) = -a/2 \times x^2 + b/4 \times x^4$. Without the bias of external forcing, the outcome state will cross the potential barrier to switch among two stable states $x_m = \pm\sqrt{a/b}$. (b) In the case of a right-biased forcing, the left states will be more stable, and transition from right to left will occur more frequently, while the reverse transition will be hindered. (c) Similarly, in the presence of a left-biased forcing, the transition from right to left will be hindered.

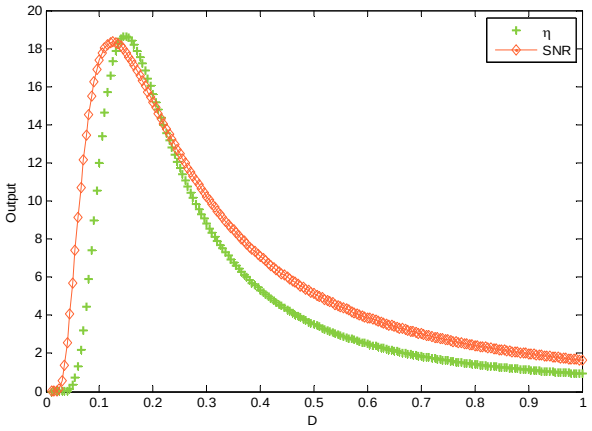

Fig. 4. The non-monotonic relationship between the output SNR/SAF and the noise variance in a non-linear SR system.

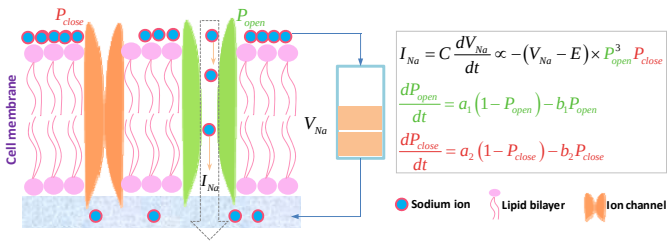

Fig. 5. Biological SR mechanisms in the voltage-gated ion channels in cell membrane. Here, the famous Hodgkin-Huxley (HH) model of the *Na* channel is considered. The voltage potential is determined by the famous Nernst equation, i.e., $V_{Na} = 62 \cdot \log(C_{\text{out}}/C_{\text{in}})$, where C_{out} and C_{in} denote the concentration of *Na* ions in outside and inside of cell membrane. The ion channels, which is highly selective for *Na*, will be opened with the probability P_{open} (e.g. the right ion channel) and closed with a probability P_{close} (e.g. the left ion channel).

2) Main Results: A detailed statistical analysis on non-linear SR can be found in survey literatures [44], [45]. Here, we focus only on the main results relevant to our non-linear filter scheme for molecular signaling.

Output response: When the above eq. (18) satisfies, the expected output of the nonlinear dynamical system, given the initial conditions $x_0 = x(t)|_{t=t_0}$ and $\varphi = 0$, is:

$$\lim_{t_0 \to -\infty} \langle x(t)|x_0, t_0\rangle = \bar{x}(D) \times \cos[\Omega t - \bar{\varphi}(D)]. \tag{19}$$

Here, $\langle x\rangle$ gives the conditional and ensemble averaging of $x(t)$ over noises [45]. From eq. (19), we note that the output response is also a periodic signal, sharing the same frequency with the weak input forcing, i.e. Ω. However, the amplitude and phase are mediated by the noise variance D as well as the underlying potential function (a and b), i.e.,

$$\bar{x}(A_0, D) = A_0 x_m^2/D \times \frac{2r_0}{\sqrt{4r_0^2 + \Omega^2}}, \tag{20}$$

$$\bar{\varphi}(D) = \arctan(\Omega/2r_0). \tag{21}$$

Output SNR: The SNR of output signal is given by [44]:

$$\text{SNR} = \frac{A_0^2}{\sqrt{2}D^2} \times \exp\left(\frac{\Delta V}{D}\right). \tag{22}$$

After passing through the non-linear dynamical system, a weak periodic (or quasi-periodic) input would be reinforced if provided a proper noise, leading to the increased output SNR. As in Fig. 4, the optimal noise variance exists which maximizes the output SNR η. By the way, we can define the ratio between the output and input amplitude as the spectrum amplification factor (SAF), and there also exists the other optimal noise variance maximizing this SAF.

Here, the SNR in (22) characterizes only the ratio of output-spectrum power between the resonance frequency (i.e. Ω) and the background noise. This is slightly different from the common SNR definition in analyzing communication systems. Note that, we only use the SNR definition in (22) to analyse the nonlinear SR filtering procedure. In the later analysis of the detection performance in molecular communications, we will focus on the common definition on SNR, i.e. the ratio between signal power and noise power.

C. Practical Implementation

Rather than directly detecting signal as in the case of binary pulse amplitude modulation (BMAP) [49], here we employ the non-linear SR mechanism to denoise molecular signals.

*1) **Analog domain implementation:*** When it comes to multi-scale molecular communications, e.g. from nano-scale (e.g. tens of nm [13]) to micro-scale (e.g. tens of μm [32], [34]) and maro-scale (e.g. several meters [5], [6]), the non-linear SR mechanism will be implemented as a part of signal receptor (see also Fig. 1-b), as a special nonlinear filter. The

implementation structure in the analog domain is shown by Fig. 6 (as for traditional linear FIR filters, once the coefficients have been determined, the physical implementation of such analog SR structures is straightforward). As seen, after the diffusive propagation and noise contamination, a received signal $y(t)$ (or y_k) will be directly fed to a well-tuned SR system. Then, its output $x(t)$ (or x_k) would be treated as a noise-reduced and signal-enhanced version of received signal.

From the analog structure, the SR mechanism can be realized simply, which, for example, involves a differentiator, an adder, two amplifiers and a power operator. Compared with traditional linear filters, the computation complexity (e.g. long-tap linear convolution) would be effectively reduced by our SR-based nonlinear filter. More importantly, in contrast to linear filters which only removes part of noise (accompanying useful signal out of the pass-band), such a nonlinear filter can even convert noise into target signals and thereby greatly enhance the output SNR.

In the biological context, non-linear SR mechanisms occur widely [46] and have more elegant realizations. For example, relying on the kinetics of successive chemical reactions (i.e. involving a group of differential equations), ion channels of cell membrane can amplify the signaling *in vitro* even in harsh biological environments with the help of noise effects, as illustrated by Fig. 5. Note that, other non-bistable systems are also demonstrated to exhibit SR effects (amplifying signal via noise), e.g. involving excited state. Examples include electron paramagnetic resonance and etc., see ref. [44] for details.

Although the controllable chemical reactions provide the insight for the future realization of SR-inspired signal processing, at the current stage we focus on its engineered application (i.e. multi-scale molecular communication via diffusion), targeting at an alternative signal detector inspired by such biological mechanisms. And, the chemical-reaction realization of nonlinear SR process is out of the scope of this work, which remains an open issue for future studies.

*2) **Digital domain Implementations**:* In other molecular communications, the digital implementation would be preferable, e.g. when developing a non-linear filter in small-size chips. In this case, one has to solve the SPDE in Eq. (17), probably with the aid of iterative computation. To accomplish this, we employ the fourth-order Runge-Kutta method (RKM) [47], which numerically approximates the solution.

Relying on the mean value theorem of difference (MVTD), the RKM manages to approximate the next output $x_{k+1} = x[(k+1)\Delta t]$ via the current one $x_k = x(k\Delta t)$, i.e., $x_{k+1} - x_k = x'(\varepsilon)\Delta t$ with $\varepsilon \in [k\Delta t, (k+1)\Delta t]$. Let $\rho = \Delta t$, then the derivative $x'(\varepsilon)$ will be estimated via a weighted average of four increments, i.e., $q_1 = f(t_k, x_k) = dV(x)/dx$, $q_2 = f\left(t_k + \frac{\rho}{2}, x_k + \frac{\rho}{2}q_1\right)$, $q_3 = f\left(t_k + \frac{\rho}{2}, x_k + \frac{\rho}{2}q_2\right)$ and $q_4 = f\left(t_k + \frac{\rho}{2}, x_k + \frac{\rho}{2}q_3\right)$, via the following equation:

$$x_{k+1} = x_k + \frac{1}{6} \times (q_1 + 2q_2 + 2q_3 + q_4), \tag{23}$$

where each increment term is calculated via:

$$q_1 = \rho \times (ax_k - bx_k^3 + y_k), \tag{24}$$

$$q_2 = \rho \times \left[a \cdot \left(x_k + \frac{q_1}{2}\right) - b \cdot \left(x_k + \frac{q_1}{2}\right)^3 + y_{k+1}\right], \tag{25}$$

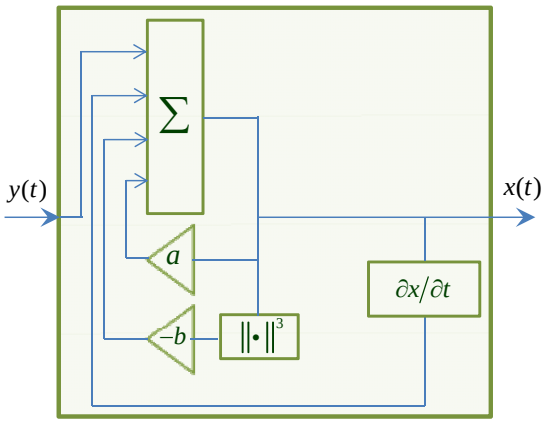

Fig. 6. A schematic structure of SR-based non-linear filter, which is implemented in the analog domain.

$$q_3 = \rho \times \left[a \cdot \left(x_k + \frac{q_2}{2}\right) - b \cdot \left(x_k + \frac{q_2}{2}\right)^3 + y_{k+1}\right], \tag{26}$$

$$q_4 = \rho \times \left[a \cdot \left(x_k + \frac{q_3}{2}\right) - b \cdot \left(x_k + \frac{q_3}{2}\right)^3 + y_{k+1}\right]. \tag{27}$$

As seen, the iteration step ρ should be related to a sampling time. The higher the sampling rate, the smaller the iteration step, and the smaller the residual error (e.g. roughly measured by $o(\rho^5)$). Thus, a compromise should be made between the estimation accuracy and the processing speed, as a small ρ may lead to slow update and immature convergence result.

D. Output Analysis

The output signal after non-linear filtering is shown in Fig. 2-(b). We note that the output noise has been suppressed effectively. And moreover, in contrast to the outputs of a linear filter where the local disjunction of input signals may have been smoothed out, subtle transient features that are of significance to subsequent information demodulation are perfectly preserved.

In addition, we observe from Fig. 7 that the output response may have been expanded, compared with an input narrow pulse, i.e. $w(t)$. It should be noteworthy that, in the context of signal detection, most previous works focus on the zero-mean and single-frequency input signal or BPAM signals [49], where the output signal directly corresponds to the detection result. Unfortunately, here the molecular signal is neither zero-mean nor involving only single-frequency signal, and thus its output has been rarely analysed in the literature, including our conference version [22]. In the following, we provide a profound theoretical and numerical analysis on the output response after the non-linear filtering process.

First, we expand the input signal $y(t)$ into Fourier series:

$$y(t) \simeq \bar{A} + \sum_{n=1}^{N_f} A_n \cos(n\Omega t) + \sum_{n=1}^{N_f} B_n \sin(n\Omega t), \tag{28}$$

where $N_f > 1$ denotes the analysis order; $\bar{A} \triangleq \frac{2}{T_\Omega} \cdot \int_0^{T_\Omega} y(t)dt$,

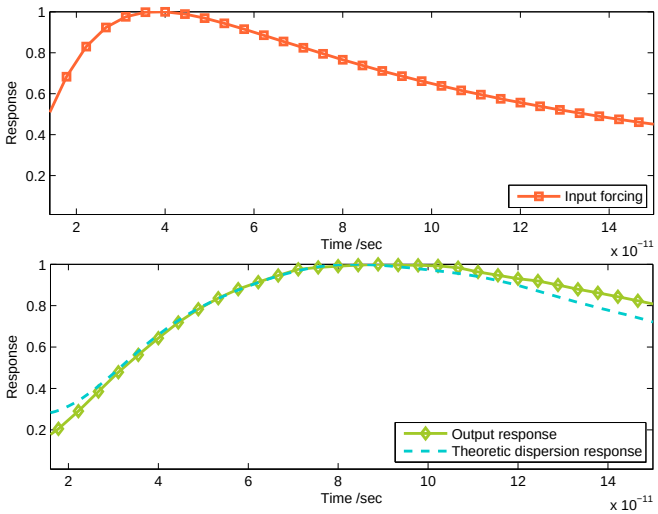

Fig. 7. The output response after the non-linear filtering. In analyzing the dispersed response, the Fourier-series order is N_f=8. *(Top)*: Normalized input response. *(Bottom)*: Normalized output response.

while other coefficients of Fourier series are computed via:

$$A_n = 2/T_\Omega \times \int_0^{T_\Omega} y(t) \cdot \cos(n\Omega t)dt,$$
$$B_n = 2/T_\Omega \times \int_0^{T_\Omega} y(t) \cdot \sin(n\Omega t)dt.$$

Then, from the previous analysis, each periodic component of frequency $n\Omega$ produces also a periodic output component with the same frequency, with its amplitude and phase determined by:

$$\bar{x}_n(A_n, D) = A_n x_m^2/D \times \frac{2r_0}{\sqrt{4r_0^2 + n^2\Omega^2}},$$
$$\bar{\varphi}_n(D) = \arctan(n\Omega/2r_0).$$

Here, we have $D = \sigma_z^2$. Since the input signal is weak, then the mutual coupling among such frequencies can be reasonably ignored. Thus, the output signal is approximated by a summation of N_f single-frequency terms, i.e.,

$$x(t) \simeq \sum_{n=0}^{N_f} \bar{x}_n(A_n, D) \times \cos[n\Omega t - \bar{\varphi}_n(D)] + \sum_{n=0}^{N_f} \bar{x}_n(B_n, D) \times \sin[n\Omega t - \bar{\varphi}_n(D)]. \quad (29)$$

From previous eqs. (20) and (21), we find that the higher the input frequency, the smaller the output amplitude, and the larger the additive phase. To this end, the *dispersion* effect will occur after molecular signals have passed through a dynamical SR system, and the output response will be stretched. From the numerical result in Fig. 7, the dispersion response derived from our theoretical analysis agrees with the observed output.

E. Parameters Adaption

In order to achieve the promising performance, the parameters of non-linear SR system should be properly tuned [48], [49], when the noise variance D is perfectly known. Intuitively, in order to assist the outcome state crossing a potential barrier, the following relationship is supposed to meet:

$$\Delta V = a^2/4b \leq D.$$

As suggested, the amplitude of input periodic forcing will also affect the behaviors of SR systems [48], which should satisfy the following constraint:

$$A_0 \leq \sqrt{4a^3/(27b)}. \quad (30)$$

Thus, considering a special case of $A_0 = 0.5 \times \sqrt{4a^3/(27b)}$ and $\Delta V = D$, the feasible parameters can be configured as:

$$a = \frac{27 \times (2A_0)^2}{16D}, \; b = \frac{a^2}{4D}. \quad (31)$$

Note that, for the concerned molecular signal (which is always positive), we would approximate the signal amplitude with $A_0 \simeq \mathbb{E}\{y(t)\}$. Meanwhile, it may become impossible to know a realistic noise variance. As an alternative, one may tend to the performance optimization in the case of high SNRs (e.g. SNR*=4dB), and then the noise variance in the above Eq. (31) will be prescribed to $D = D_{\text{est}} = 10^{-\frac{\text{SNR}^*}{10}} \times A_0$.

IV. CSI-independent Detection

After the non-linear filtering, we then recover unknown information via a simple CSI-independent and non-coherent detector. The main motivation of our designed CSI-independent detector will be two-fold. First, the estimation of diffusion channel responses inevitably consumes considerable time or energy resources, and more importantly, subsequent coherent detection (i.e. MAP or MMSE) even becomes computationally unaffordable for nano-machines. Second, although the additive noise has been suppressed effectively via the non-linear filtering, the output dispersion response will be quite different from an input response and, consequently, the coherent detection may be intractable even CSI (i.e. $w(t)$) can be available.

A. Metric Construction

In our non-coherent detection framework, the decision metric will be constructed directly from the filtered waveform $x(t)$ (or x_n), which completely excludes the estimated CSI. Since the analytic expression of output response is intricate, the following analysis focuses on the whole **transient feature** of $x(t)$. To be specific, we firstly construct three decision sub-metrics by respectively exploring: (1) the local geometry shape in each symbol, (2) the transient property among two adjacent symbols, and (3) the energy difference between two symbols. Note that, such a transient-feature based detection concept is also inspired by biological mechanisms in cell signaling, for example, the different concentration gradient slopes may represent different information and thereby trigger various biological responses [50].

*1) **Local geometry shape**:* Taking the kth interval with $M = T_b f_s$ samples for example, see Fig. 8-(a), in the case of H_1 (i.e. α_k=1) the output response $x(n)$ will firstly arise until its maximum (located at $M_x \triangleq kM + M_{\max}$), then it will decay slowly. Thus, the output response in a region $\mathcal{R}_2$ will be higher than both its left neighbor region $\mathcal{R}_1$ and right neighbor $\mathcal{R}_3$. In practice, we will specify the width of peak convexity region $\mathcal{R}_2$ to be M/4+1, i.e. the half length is $L_0 = M/8$ (see Fig. 8-a). Different from our previous convexity metric [16], the first sub-metric excludes the inflection point information and is defined as:

$$c_{k,1} = \frac{1}{2L_0+1} \cdot \sum_{n=M_x-L_0}^{M_x+L_0} x_n - \frac{1}{2} \cdot \frac{1}{M-2L_0-1} \cdot \left(\sum_{n=kM}^{M_x-L_0-1} x_n + \sum_{n=M_x+L_0+1}^{(k+1)M-1} x_n \right). \tag{32}$$

It is easily noted that, in the case of H_1 (i.e. α_k=1), $c_{k,1}$ will be larger than 0. Otherwise, noted also from Fig. 8-(a), it may become smaller than 0 in the other case of H_0 (i.e. α_k=0). So, it can be indeed used as a metric to justify whether there are new molecules (i.e. α_k=1) arriving at a receptor at the current symbol interval.

*2) **Transient shape among symbols**:* When it comes to two successive slots k and $k+1$, the transient shape at the beginning of the next symbol (i.e. kM) will be quite different in two cases (i.e. H_1 and H_0), see Fig. 8-(b). To be specific, in the case of H_0 (α_k=0), the output response will continue to decay in the following time. In contrast, for H_1 (α_k=1) an obvious inflection may occur. To exploit such a transient pattern, another sub-metric is formulated as:

$$c_{k,2} = \frac{-1}{2L_1+1} \cdot \sum_{n=kM-L_1}^{kM+L_1} x_n + \frac{1}{2} \cdot \frac{1}{2L_2+1} \cdot \left(\sum_{n=kM-L_1-L_2}^{kM-L_1-1} x_n + \sum_{n=kM+L_1+1}^{kM+L_1+L_2} x_n \right). \tag{33}$$

where L_1 and L_2 represent respectively the width of transient sub-region and neighboring sub-regions within $\mathcal{R}_4$ (see Fig. 8-b). L_1 is practically configured to a small value, e.g. $L_1 = 1$.

*3) **Energy difference**:* Except for the above two geometry sub-metrics, another differential metric developed in [7] can be also applicable, which utilizes the concentration difference induced by the new arrived molecules and exploits the slow-decay property of diffusion channels. Thus, the third sub-metric is specified as:

$$c_{k,3} = \frac{1}{M} \cdot \sum_{n=kM+1}^{(k+1)M} x_n - \frac{1}{M} \cdot \sum_{n=(k-1)M+1}^{kM} x_n. \tag{34}$$

Finally, our compound non-coherent metric is defined as:

$$c_k = c_{k,1} + c_{k,2} + c_{k,3}. \tag{35}$$

As elaborated above, the designed sub-metrics are consistent in detecting new arrived molecules, i.e., $c_{k,i} \underset{\alpha_k=1}{\overset{\alpha_k=0}{\lessgtr}} \lambda_i$ ($i = 1, 2, 3$), where λ_i are detection thresholds. More importantly, with the independent noise samples, the combination of the above three sub-metrics may even provide certain diversity gain in detection performance.

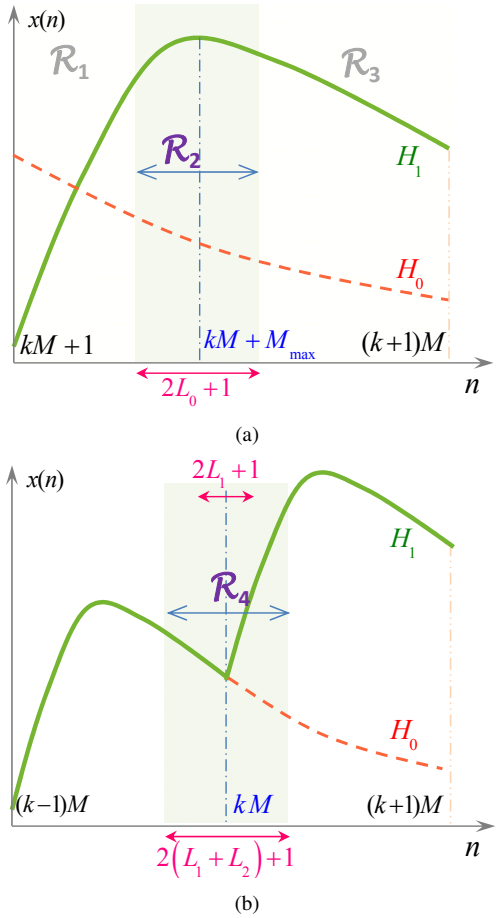

Fig. 8. Non-coherent metrics based on the geometry characteristic of the filtered response. (a) The local convexity metric, in each symbol duration $[kM+1, (k+1)M]$, will be larger than zero in the case of H_1, as demonstrated by the $\mathcal{R}_2$ region of the green solid curve. In contrast, it will be smaller than zeroes in the case of H_0, as shown by the $\mathcal{R}_4$ region of the red dotted curve. (b) The transient metric among two adjacent symbols. In the case of H_1, the inflection transient shape can be observed, while the smooth decay transient shape will be observed in the case of H_0.

Of course, the weighted metric combination, rather than the above equal ratio combination (ERC), will obtain the additional gain. One can refer to ref. [53] for more details, whilst our emphasis in this work is put on the nonlinear detection process and hence an ERC scheme is used.

B. Detection Threshold

The mean of the above non-coherent metric in the case of H_1, i.e. $\mathbb{E}(c_k|H_1, t_0 \to -\infty) = E_1$, will be related with the specific shape of an output response $x(n)$ as well as the ISI. As the noise samples of various discrete time remains independent, c_k will be Gaussian distributed when the sample size M is sufficiently large (e.g. $\geq$20), according to the central limit theorem (CLT). Conditioned on different cases (i.e. H_1

or H_0), the likelihood densities of our designed metric are:

$$p(c_k|H_1, t_0 \to -\infty) \sim \mathscr{N}(E_1, \sigma_c^2), \tag{36}$$
$$p(c_k|H_0, t_0 \to -\infty) \sim \mathscr{N}(E_0, \sigma_c^2). \tag{37}$$

Here, $E_0 \triangleq \mathbb{E}(c_k|H_0, t_0 \to -\infty)$ and the distribution variance σ_c^2 will be related with the sample size M, and the residual noise variance in x_k (whose value is hard to determine even we can know the noise variance σ_z^2).

Then, a threshold λ can be derived according to certain criterion, e.g. the minimum detection errors (MDE), with which the estimation of unknown symbols is derived via:

$$\hat{\alpha}_k = \begin{cases} 1, & c_k \geq \lambda, \quad (38a) \\ 0, & c_k < \lambda. \quad (38b) \end{cases}$$

Taking the equal prior information symbols for example, i.e. $p(H_1) = p(H_0) = 0.5$, the optimal threshold under an MDE criterion is supposed to meet:

$$\lambda_{\text{opt}} = \arg\min_{\lambda \in \mathbb{R}^1} \left\{ p(H_1) \times \int_{-\infty}^{\lambda} p\{c(x)|H_1, t_0 \to -\infty\} dc(x) + p(H_0) \times \int_{\lambda}^{\infty} p\{c(x)|H_0, t_0 \to -\infty\} dc(x) \right\}. \tag{39}$$

Replacing the Gaussian likelihood distributions of Eqs. (36)-(37) into the above equation[2], then the optimal threshold is determined by:

$$\begin{aligned} \lambda_{\text{opt}} &= 0.5 \times (E_1 + E_0) = p(H_1) \cdot E_1 + p(H_0) \cdot E_0, \\ &= \int_0^{\infty} c(x) p\{c(x)|t_0 \to -\infty\} dc(x). \end{aligned} \tag{40}$$

C. Threshold Estimation

An analytic form of the above threshold can be hardly obtained, due to the non-analytic response x_k and the noise variance σ_c^2 of the non-coherent metric. Alternatively, at the kth interval we may evaluate the threshold adaptively, by utilizing the constructed non-coherent metric $c_{1:k}$. One direct approach is to update the threshold adaptively according to:

$$\lambda_k = (1 - \beta) \times \lambda_{k-1} + \beta \times \frac{1}{k} \sum\nolimits_{k'=1}^{k} c_{k'}, \tag{41}$$

where β is a forgotten parameter which is ranged in $[0.9, 0.99]$; an initial threshold estimation can simply be set to $\lambda_0 = 0$. It is shown that, as an iteration number k increases, the estimated threshold will converge to its real value, i.e.,

$$\begin{aligned} \lim_{k \to \infty} \lambda_k &= \frac{1}{k} \sum\nolimits_{k'=1}^{k} c_{k'} \simeq \mathbb{E}(c_k), \\ &= p(H_1) \times \mathbb{E}(c_k|H_1) + p(H_0) \times \mathbb{E}(c_k|H_0), \\ &= \lambda_{\text{opt}}. \end{aligned} \tag{42}$$

[2]Here, even if the additive noise $z(t)$ is not Gaussian distributed, the likelihood density may be still approximated via a Gaussian distribution (when M is large). This is because the construction of CSI-independent sub-metrics involves the summation of many independent noise samples.

D. Implementation Considerations

1) Implementation: The proposed scheme involves three successive steps: (1) SR-based **nonlinear filtering**, (2) non-coherent **metric computation** and (3) threshold-based **detection**. For each component, we have discussed the implementation structure from an engineering point of view, e.g. both the analog implementation of nonlinear filtering in Fig. 6 and the digital implementation in eqs. (23)-(27).

One important problem in real application is the selection of CSI-independent metrics. Here, we only construct three metrics by fully utilizing the transient feature of received signals. Yet, its optimality can be hardly justified, since it utilizes no knowledge of CSI and we have no criterion to strictly define the optimality. In fact, such transience-based information detection has been widely emerged in biological process [3], [50] (e.g. different transient patterns or slopes may lead to different responses), whereby the reliability and low-complexity would be the primary goal (rather than the optimality). In the presence of the perfect CSI, then the achievable lower bound of our non-coherent method is obtained by the MAP detector, which is able to exploit the whole information rather than the local transient features.

2) Implementation Complexity: Based on the above analysis, the complexity of our proposed scheme involves three parts. At the nonlinear filtering stage, the main computation comes mainly from the approximated solution of Eq. (17). According to Eqs. (23)-(27), for each sampling time k, total 27 multiplications are required (when the digital implementation is used). In the second stage, for each symbol 6 multiplications are required to calculate a decision variable, see Eqs. (32)-(34). In the final stage, 3 multiplications are required to update the threshold, see Eq. (41). Thus, the total complexity is roughly measured by $\mathcal{O}(KM)$, which is significantly lower than the coherent MAP and MMSE detectors (if the complicated CSI estimation is further considered) [13], [16].

V. NUMERICAL RESULTS

In this Section, we evaluate the detection performance of our proposed CSI-independent non-linear signal processing scheme. In the numerical simulation, we configured the diffusion constant to $C = 89.4 \times 10^{-12}\text{m}^2/s$, and the transmitter-receiver (T-R) distance is $d = 20 \times 10^{-6}$m [39]. The sampling time is $T_s = 1/f_s = 2 \times 10^{-10}$ sec, and the symbol interval of binary information is 7.5×10^{-2} sec (i.e. the discrete samples within each symbols duration is M=45). Note that, in the following the SNR is defined as the ratio of signal and noise power, which differs from eq. (22). The mean value of received signals was estimated by averaging the arrived molecular messengers.

A. Adaptive Threshold

In the first simulation, we studied the designed adaptive threshold mechanism. As in Fig. 2-(b), the output SNR of filtered signals after passing a nonlinear dynamical system) will be remarkably improved, by constructively utilizing random noise. Then, the non-coherent detection metrics will be constructed via Eqs. (32)-(35). When the input SNR is

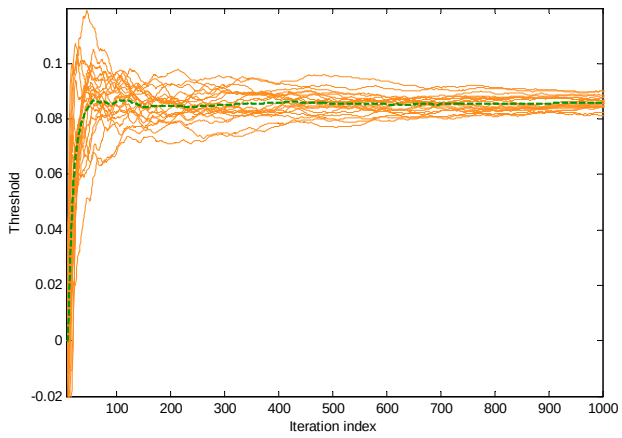

Fig. 9. The threshold adaption in 25 independent realizations.

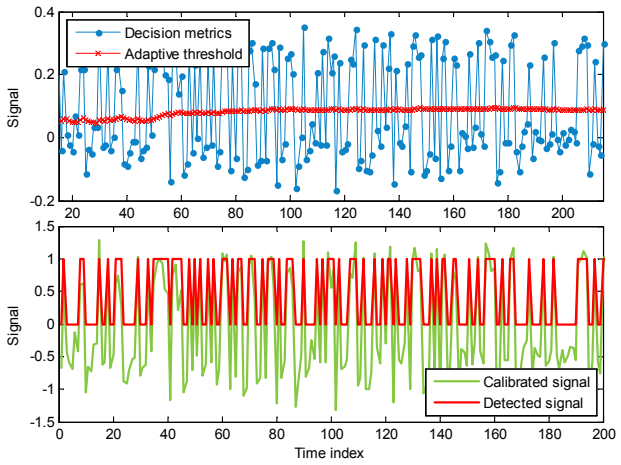

Fig. 10. *Top*: The derived non-coherent metrics as well as the adaptively updated threshold. *Bottom*: The calibrated signal, i.e. $c_k - \mathbb{E}(c_k|t_0 \to \infty)$, and the decision results. Here, the input SNR is configured to 8dB.

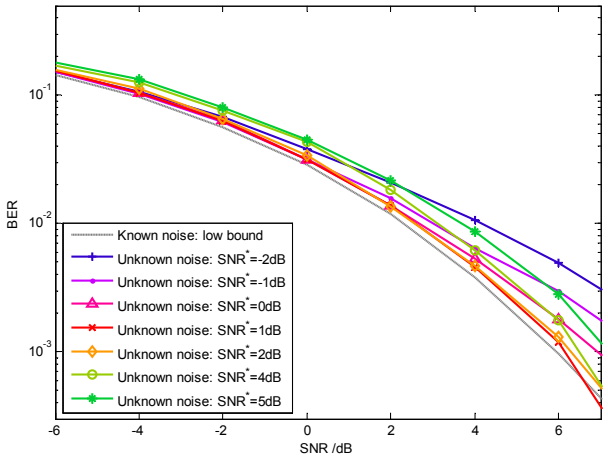

(a)

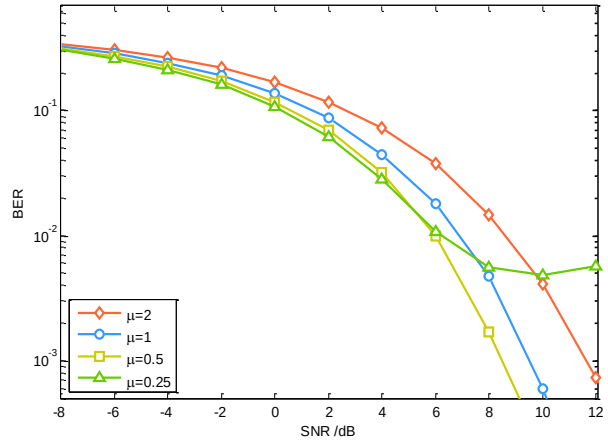

(b)

Fig. 11. BER performance with various parameter configurations. (a) Effects from the configuration of the double-well potential, i.e. a and b, in the presence of various predefined SNRs. (b) Influences from the scaling factor (or the iteration step).

configured to 8dB, the adaptive threshold obtained from 25 independent realizations are plotted in Fig. 9. It is seen that the threshold can be acquired numerically via the decision variable c_k ($k = 0, 1, 2, \cdots, K-1$), and its convergence can be achieved after around 30∼40 symbols (leading to a short start-up time). It is shown that, from Fig. 10, unknown binary signals can be detected correctly via this automatic threshold. That is, with the proposed non-coherent decision variable and the adaptive threshold, our method is able to exclude the explicit CSI and its complex estimation process.

B. Parameters Configuration

We then investigated the influences of the parameter configuration in non-linear detector. When the channel noise is exactly known by a molecular receptor, the promising detection performance can be attained by properly configuring the parameters in Fig. 6 (analog implementation) or Eqs. (23)-(27) (digital implementation). In the absence of exact noise variance, one can configure the potential parameters according to a *predefined* SNR. The detection performance with various predefined SNRs (i.e. the real noise variance is unknown) is plotted in Fig. 11-(a). When the predefined SNR is too small (e.g. SNR*=-2dB), it results in a much larger noise variance $D_{\text{est}} = 10^{-\text{SNR}^*/10} \times A_0$, and thereby specifies a higher potential barrier ΔV, which may prohibit the noise-aided transition among two stable states. While a too large predefined SNR (e.g. SNR*=5dB) leads to the small noise variance D_{est} and much lower potential barrier ΔV, which facilitates in excess the noise-aided transitions (also see Fig. 4). From simulation analysis, the feasible range of a predefined (or realistic) SNR will be $\text{SNR}^* \in [1,\ 4]$dB. Without losing the generality, in following analysis we assume the noise variance remains unknown, which is then estimated via the proper predefined SNR*=4dB. Note that, in this case the detection performance may be slightly degraded, compared with a known noise variance. Even so, the off-line parameter configuration of our proposed method is feasible in practice.

We also studied the influence of an iteration step (i.e. ρ) for the RKM method when numerically solving a nonlinear SR system. As indicated, a small iteration step ρ leads to the smaller residual error of nonlinear filtering and thereby the better detection performance, as shown in Fig. 11-(b).

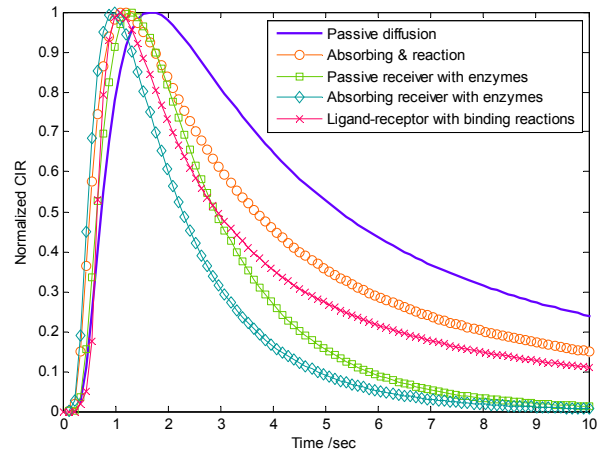

(a)

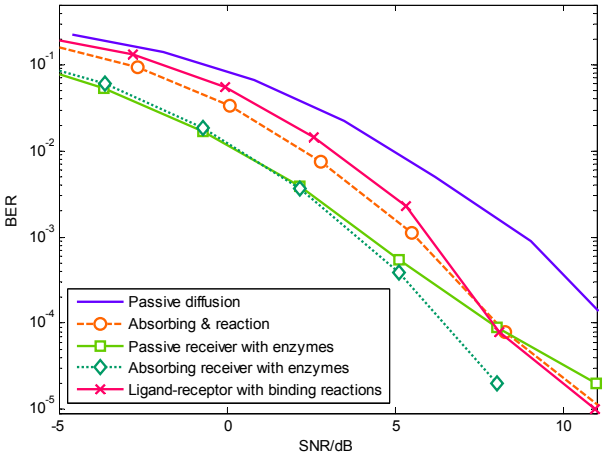

(b)

Fig. 12. (a) The expected molecular concentrations or CIRs of different types of receiver. Here, the diffusion constant is $D = 89.4 \times 10^{-12}$ m^2/s, the T-R distance is $d = 30 \times 10^{-6}$m and the sampling time is $T_s = 1 \times 10^{-1}$ sec. Other specific parameters can be found in refs. [32], [34], [36]. (b) BER performance of our proposed non-coherent detector in the presence of various CIRs ($M = 45$). When applied to other receivers, no further adjustment was made to the designed non-coherent detector.

Here, we assume the iteration step has been normalized by a sampling time, i.e. $\rho = \mu/M$. From the numerical result in Fig. 11-(b), if a scaling factor μ is reduced from 2 to 0.5, the rough detection gain of 3dB can be obtained. However, such a parameter should be configured carefully in practice. E.g., if further reducing the scaling factor to 0.25, then an error floor will occur, by seriously deteriorating the detection performance. Thus, in the high SNR region (e.g. SNR>6dB), a too small iteration step can't help but degrade the performance. This is because, with time-varying input signals, the iterative computation may be far from convergence when using a too small step, which may hence produce inaccurate output.

C. Practical Considerations

As noted from the designing of our non-coherent detector, it should be independent of a specific type of receiver, e.g. passive receiver, absorb receiver, passive/absorb receiver with enzyme, or ligand receptor with binding behaviors. In essence,

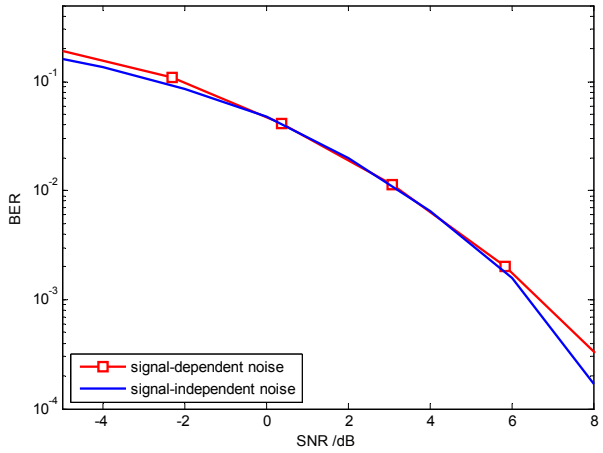

Fig. 13. Detection performance of our proposed non-coherent detector with different signal noise modeling.

it detects unknown information directly via the transient trend of dynamical molecular concentration; whist such a trend of first-rising-then-decaying is prevalent in various receivers of different CIRs, as in Fig. 12-(a). Therefore, our new scheme can be directly extended to other types of receivers (note that, in this case the algorithm configuration needs no further change). From Fig. 12-(b), it is also seen that the Passive receiver can be used as the benchmark in performance evaluation, as it has the slowest rising and decay profile, thereby resulting in the most serious ISI and the largely degraded BER.

Meanwhile, our designed non-coherent detector is also independent of various additive noises. As discussed, the signal-independent noise can be used in designing the robust non-coherent detector, whereby neither the statistical distribution (i.e. Gaussian or Non-Gaussian) nor the time-varying variance is required. As expected, it is thereby applicable to signal-dependent noise. From Fig. 13, the BER performance in the case of signal-dependent noise will be degraded slightly in the same SNR. This is mainly because, with the signal-dependent noise, the nonlinear SR mechanism should be adapted according to the time-varying noise variance, in order to produce the optimal performance. However, this should result in the less robust detector in practical MC systems. In contrast, the signal-independent noise allows to the design of non-optimal yet robust non-coherent detector, which could operate well even in the presence of signal-dependent noise.

Besides, we note that, in the case of imperfect timing, the detection performance of our non-coherent detector will be slightly affected. From Eqs. (32)-(35), the only required information is the deviated location of peak concentration, i.e. M_{max}. So, in practice we can reasonably assume the symbol duration can be known as *a priori*, whist the imperfect synchronization may lead to another deviated sample sequence (with another deviated peak). Yet, the location of maximum peak concentration can be directly estimated. Even when the deviated estimation of the peak concentration occurs, the detection performance will be slightly degraded, as shown in Fig. 14. Thus, as one inherent merit, this CSI-independent detector is essentially immune to imperfect timing.

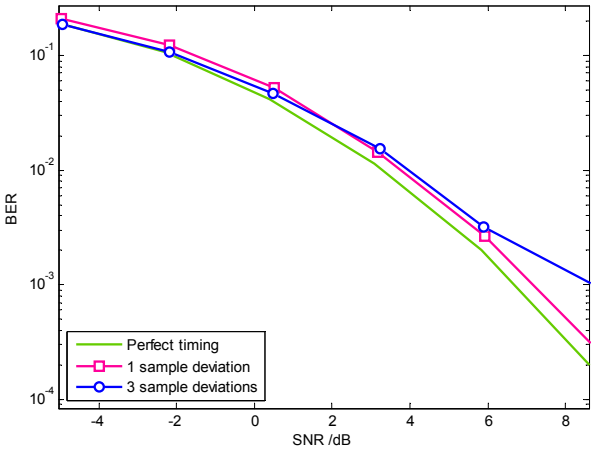

Fig. 14. Detection performance of our proposed non-coherent detector with different accuracy of timing.

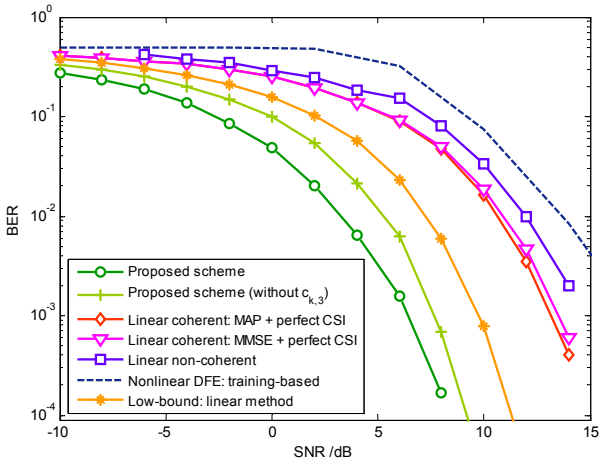

Fig. 15. Detection performance of various linear/non-linear and coherent/non-coherent schemes.

Lastly, although we focus on the concentration modulation method in the analysis, our developed nonlinear and non-coherent detector is readily applicable to other modulation formats, e.g. timing or molecular-type modulations. Taking the molecular-type modulation for example, after the reception of molecule messengers, two separated signals would be obtained, e.g. by using the type-specific sensors. Thus, such two signals can be processed successively, e.g. including nonlinear filtering and non-coherent detection, and finally, we obtain the detection result by combining two outputs. Similarly, our method can be also applied to the timing modulation method.

D. Performance Comparison

Finally, we study the detection performance of our scheme and other methods. In this simulation, we consider the existing linear (e.g. MAP) and nonlinear (i.e. DFE), coherent (based on CSI estimation) and non-coherent (without CSI estimation) detectors for the comprehensive comparison. For the MAP scheme, we assume the diffusive CSI $w(t)$ has been perfectly estimated, which of course consumes the considerable time (e.g. dedicated pilots carrying no information is required to estimate CSI) and computation resource (e.g. frequently computing likelihood functions). In the simulation, the sample interval is set to M=45. For the non-coherent detector [16], the local smoothing length is set to 12 samples.

From Fig. 15, we may firstly note that, in the linear processing framework, the MAP detector obtains the optimal performance (whereby the perfect CSI was assumed), as it has fully exploited the statistics of observations as well as CSI. However, it requires an accurate CSI estimation and complex computation (even with a truncated ISI length, e.g. $I = 30$), which thereby becomes less attractive, especially in low-power and low-complexity applications (e.g. nano-machines). The linear non-coherent detector, developed in ref. [16] and relying similarly on the convexity shape of molecular concentration, will effectively alleviate the computation burden, and hence is more applicable in low-complexity scenarios. It is seen that both two linear detectors acquire satisfactory performances only in high SNRs (e.g. >12dB), which, unfortunately, becomes impractical in noisy biological environments that are ubiquitous in nature. Besides, for such linear detectors, an un-achievable low bound on BER is also provided, which corresponds to the theoretical performance of OOK modulation in Gaussian channel (i.e. the ISI effect has been completely removed). Due to the residual ISI, there is yet an obvious gap between linear methods and this low-bound.

We then evaluated the performance of nonlinear DFE [13], [18]. In the simulation, we set the step size in norm-LMS to $\mu = 0.04$, the tap length of feed-forward and feedback filter are $L = 10$ and $B = 9$, respectively. The training length is 2000 symbols. From Fig. 15, we found that the nonlinear DFE is inferior to the linear MAP. This is because, despite the nonlinear mechanism, the DFE would estimate the inexplicit channel response and is thereby sub-optimal. One major merit of nonlinear DFE is that the detection complexity will be noticeably reduced, yet at the expense of the energy-demanding training symbols.

In comparison with aforementioned schemes, our proposed nonlinear non-coherent detector may provide the great promise to molecular communications. For one thing, it excludes complicated CSI estimations and complex computations. Further considering the non-linear mechanism that can be accomplished via biological activities (as in Fig. 5), e.g. successive chemical reactions [51] or analog feedback controlling [52], the implementation will be very simple, which greatly facilitates the emerging nano-scale communications. For another, the random noise can be now utilized constructively (after converted to useful signals), which further contributes to improve the output SNR. Thus, the nonlinear filtering dramatically outperforms the existing linear filtering schemes. From the numerical result in Fig. 15, a rough detection gain of 7dB can be achieved by the proposed nonlinear non-coherent detector. Hence, our new paradigm is of significance to molecular communications, especially in harsh biological conditions.

Besides, we note that the designed compound metric, which involves both the convexity sub-metric (i.e. $c_{k,1}$) and the difference sub-metric (i.e. $c_{k,3}$), can outperform the single

convexity metric (i.e. $c_{k,1}$), as in Fig. 15. This indicates that, even without a multiple-input multiple-output configuration that will be hardly deployed in open diffusive environments, a certain degree of detection diversity can be achieved via the well-designed sub-metrics.

To this end, we argue that, after the long-term self-adaption and evolution, biological systems have created their own elegant processing mechanisms. Although some of them remain largely elusive, such methods, e.g. usually nonlinear and complex, have made great successes in various noisy biological environments. In some applications, applying the common concepts/techniques developed for artificial communication systems directly to molecular communication will be proved of little avail, or even might trigger just the opposite effect (e.g. increased complexity and limited performance). Our proposed nonlinear filter and non-coherent detector, as one of the first attempt to process molecular signals from an entirely biological point of view, have got the remarkable achievements.

VI. Conclusions

Molecular communications constitute a new framework of multi-scale information transfer. The underlying communication process faces the challenge of robust signal detection in complex diffusive channels. Applying existing techniques developed for telecommunications (usually linear or CSI-dependent) directly will be infeasible to the envisaged low-complexity nano-scale applications, whereby SNR is low and the diffusion channel is unknown. Inspired by the biological principles, we proposed a non-linear non-coherent signal processing framework with the low implementation complexity. The concept of SR is exploited to perform non-linear filtering, which can both filter out noise and transform the noise into useful signals via tailored non-linear dynamics. Thus, the output SNR will be significantly improved, and we shown the significant improvement over coherent optimal detector.

To complement the SR detector, we also design a novel non-coherent scheme, which fully utilises the transient features of filtered responses. The results show the reliable detection of molecular signals can be accomplished with a relatively low complexity, while the detection performance can be improved dramatically compared with the optimal coherent detector used in telecommunications. Despite the great potential, many open topics on such nonlinear and non-coherent detectors, e.g. the designing of non-coherent metrics, the optimal combination of multiple metrics, the maximum enhancement of output SNR and the achievable/unachievable lower bound on BER, remain unsolved and may be investigated in future. Even so, we argue that our new nonlinear processing scheme opens up the new prospect for the designing of biological information detection techniques, which are oriented to noisy biological environments and may shed light on improving the design of EMW-based communications.

Acknowledgment

This work was supported by the Young Talent Lifting Program of China Institute of Communications under Grant QT2017001, National Natural Science Foundation of China (NSFC) under Grant 61971050.

References

[1] T. D. Wyatt, “Fifty years of pheromones,” *Nature*, vol. 457, 2009, pp. 262-263.

[2] I. F. Akyildiz, F. Brunetti, C. Blázquez, “Nanonetworks: A new communication paradigm,” *Comput. Netw. (Elsevier) J.*, vol. 52, pp. 2260-2279, Aug. 2008.

[3] J. Purvis, and G. Lahav, “Encoding and Decoding Cellular Information through Signaling Dynamics,” *Cell*, vol. 152, no. 5, 2011, pp. 945-956.

[4] G. Micali, G. Aquino, D. M. Richards, R. G. Endres, “Accurate encoding and decoding by single cells: amplitude versus frequency modulation,” *PLOS Computational Biology*, vol. 11, no. 6, 2015.

[5] W. Guo, C. Mias, N. Farsad, and J. L. Wu, “Molecular versus Electromagnetic Wave Propagation Loss in Macro-Scale Environments,” *IEEE Transactions on Molecular, Biological and Multiscale Communications*, vol. 1, no. 1. 2015, pp. 18-25.

[6] N. Farsad, W. Guo, and A. W. Eckford, “Tabletop molecular communication: Text messages through chemical signals,” *PLOS ONE*, 2013, vol. 8, no. 12, e82935.

[7] B. Li, M. Sun, S. Wang, W. Guo, C. Zhao, “Low-complexity Non-coherent Signal Detection for Nano-Scale Molecular Communications,” *IEEE Transactions on NanoBioscience*, vol. 15, no. 1, 2015, pp. 3-10.

[8] W. Guo, T. Asyhari, N. Farsad, H. B. Yilmaz, B. Li, A. Eckford, C-B. Chae, “Molecular Communications: Channel Model and Physical Layer Techniques,” *IEEE Wireless Communications*, vol. 23, no. 4, 2016, pp. 120-127.

[9] B. Atakan, O. B. Akan, and S. Balasubramaniam, “Body area nanonetworks with molecular communications in nano-medicine,” *IEEE Communications Magazine*, vol. 50, no. 1, 2012, pp. 28-34.

[10] H. Arjmandi, A. Gohari, M. N. Kenari, and F. Bateni, “Diffusion-based nanonetworking: A new modulation technique and performance analysis,” *IEEE Communications Letters*, vol. 17, no. 4, 2013, pp. 645-648.

[11] C. Kearney and D. Mooney, “Macro-scale delivery systems for molecular and cellular payloads,” *Nature Materials*, vol. 12, 2013, pp. 1004-1017.

[12] A. Noel, K. C. Cheung, and R. Schober, “Joint channel parameter estimation via diffusive molecular communication,” *IEEE Transactions on Molecular, Biological and Multi-Scale Communications,* vol. 1, no. 1, pp. 4C17, Mar. 2015.

[13] D. Kilinc and O. B. Akan, “Receiver Design for Molecular Communication,” *IEEE Journal on Selected Areas in Communications*, vol. 31, no. 12, 2013, pp. 705-714.

[14] A. Noel, K. C. Cheung, and R. Schober, “Optimal receiver design for diffusive molecular communication with flow and additive noise,” *IEEE Trans. NanoBiosci.*, vol. 13, no. 3, 2014. pp. 350-362.

[15] L. S. Meng, P. C. Yeh, K. C. Chen, and I. F. Akyildiz, “On receiver design for diffusion-based molecular mommunication,” *IEEE Transactions on Signal Processing,* vol. 62, no. 22, pp. 6032-6044, Nov. 2014.

[16] B. Li, M. Sun, S. Wang, W. Guo, C. Zhao, “Local Convexity Inspired Low-complexity Non-coherent Signal Detector for Nano-scale Molecular Communications,” *IEEE Transactions on Communications*, vol.64, no. 5, 2016, pp. 2079-2091.

[17] I. Llatser, A. Cabellos-Aparicio, M. Pierobon, et al, “Detection Techniques for Diffusion-based Molecular Communication,” *IEEE Journal on Selected Areas in Communications*, 2014, vol. 31, no. 12, pp. 726-734.

[18] V. Jamali, N. arsad, R. Schober, et al., “Non-Coherent Detection for Diffusive Molecular Communication Systems,” *IEEE Transactions on Communications*, 2018, doi: 10.1109/TCOMM.2018.2792457, in press.

[19] M. A. Lemmon, J. Schlessinger, “Cell signaling by receptor tyrosine kinases,” *Cell*, 2010, vol. 141, no. 7, pp. 1117-1134.

[20] J. K. Douglass, L. Wilkens, E. Pantazelou, et al., “Noise enhancement of information transfer in crayfish mechanoreceptors by stochastic resonance,” *Nature*, 1993, vol. 365, no. 6444, pp. 337-40.

[21] M. Pierobon and I. F. Akyildiz, “Diffusion-based noise analysis for molecular communication in nanonetworks,” *IEEE Transactions on Signal Processing*, vol. 59, no. 6, pp. 2532-2547, Jun. 2011.

[22] B. Li, W. S. Guo, C. L. Zhao, “Non-linear Signal Detection for Molecular Communications,” in *Proc. of* IEEE Globecom, pp. 1-6, Nov. 2017.

[23] M. Pierobon and I. F. Akyildiz, “A Physical End-to-end Model for Molecular Communication in Nanonetworks,” *IEEE J. Sel. Areas Commun.*, vol. 28, no. 4, pp. 602-611, May 2010.

[24] Y. Chahibi, M. Pierobon, S. O. Song, and I. F. Akyildiz, "A molecular communication system model for particulate drug delivery systems," *IEEE Trans. Biomed. Eng.*, vol. 60, no. 12, 2013, pp. 3468-3483.

[25] N. Farsad, H. B. Yilmaz, A. Eckford, et al, "A Comprehensive Survey of Recent Advancements in Molecular Communication," *IEEE Communications Surveys Tutorials* , vol. 18, no. 3, February 2016, pp. 1-34.

[26] J. Philibert, "One and a Half Century of Diffusion: Fick, Einstein, Before and Beyond," *Diffusion Fundamentals*, 2006. 4:6.1-6.19.

[27] A. D. Polyanin, *Handbook of Linear Partial Differential Equations for Engineers and Scientists*, Chapman Hall/CRC Press, Boca Raton, 2002.

[28] E. A. Codling, M. J. Plank, S. Benhamou, "Random walk models in biology," *Journal of the Royal Society Interface*, 2008, vol. 5, no. 25, pp. 813-34.

[29] H. ShahMohammadian, G. G. Messier, S. Magierowski, "Blind synchronization in diffusion-based molecular communication channels," *IEEE communications letters*, 2013, vol. 17, no. 11, pp.2156-2159.

[30] N. Farsad, N. Kim, A. Eckford, and C. Chae, "Channel and noise models for nonlinear molecular communication systems," *IEEE Journal on Selected Areas in Communications*, vol. 32, no. 12, 2014, pp. 1-14.

[31] Andreas F. Molisch. *Wireless Communications*, 2nd Edition, Wiley Press, 2010.

[32] H. B. Yilmaz, A. C. Heren, T. Tugcu, et al., "Three-Dimensional Channel Characteristics for Molecular Communications With an Absorbing Receiver," *IEEE Communications Letters*, 2014, vol. 18, no. 6, pp. 929-932.

[33] H. B. Yilmaz and C.-B. Chae, "Arrival modelling for molecular communication via diffusion," *Electron. Lett.*, vol. 50, no. 23, pp. 1667-1669, 2014.

[34] A. C. Heren, H. B. Yilmaz, C. B, Chae, T. Tugcu, "Effect of Degradation in Molecular Communication: Impairment or Enhancement?," *IEEE Transactions on Molecular, Biological and Multi-Scale Communications*, 2014, vol. 1, np. 2, pp. 217-229.

[35] A. Noel, K. C. Cheung, R. Schober, "Improving Receiver Performance of Diffusive Molecular Communication With Enzymes," *IEEE Transactions on NanoBioscience*, vol. 13, no. 1, 2014, pp. 31-43.

[36] A. Ahmadzadeh, H. Arjmandi, A. Burkovski, R. Schober, "Comprehensive Reactive Receiver Modeling for Diffusive Molecular Communication Systems: Reversible Binding, Molecule Degradation, and Finite Number of Receptors," *IEEE Transactions on Nanobioscience*, vol. 15, no. 10, 2016, pp. 713-727.

[37] V. Jamali, A. Ahmadzadeh, R. Schober, "On the Design of Matched Filters for Molecule Counting Receivers," *IEEE Communications Letters*, 2017, vol. 21, no. 8, pp. 1711-1714.

[38] H. Shahmohammadian, G. G. Messier, S. Magierowski, "Optimum receiver for molecule shift keying modulation in diffusion-based molecular communication channels," *Nano Communication Networks*, 2012, vol. 3, no. 3, pp. 183-195.

[39] Mahfuz, Mohammad U., D. Makrakis, H. T. Mouftah, "A Comprehensive Study of Sampling-Based Optimum Signal Detection in Concentration-Encoded Molecular Communication," *IEEE Transactions on Nanobioscience*, vol. 13, no. 3, 2014, pp. 208-222.

[40] M. Abdulrahman, A. U. H. Sheikh, D. D. Falconer, "Decision feedback equalization for CDMA in indoor wireless communications," *IEEE Journal on Selected Areas in Communications*, 1994, vol. 12, no. 4, pp. 698-706.

[41] R. Benzi, A. Sutera, A. Vulpiani, "The mechanism of stochastic resonance," *Journal of Physics A: Mathematical General*, 1981, vol. 14, no. 11, pp. 453-457.

[42] R. Benzi, G. Parisi, A. Sutera, et al, "Stochastic resonance in climatic change," *Tellus*, 1982, vol. 34, no. 1, pp. 10-16.

[43] L. Gammaitoni, E. Menichella-Saetta, S. Santucci, et al., "Extraction of periodic signals from a noise background," *Physics Letters A*, 1989, vol. 142, no. 2, pp. 59-62.

[44] L. Gammaitoni, P. Hänggi, P. Jung, et al., "Stochastic resonance," *Reviews of Modern Physics*, vol. 70, no. 1, 1998, pp. 223-287.

[45] B. Mcnamara, K. Wiesenfeld, "Theory of stochastic resonance," *Physical Review A*, 1989, vol. 39, no. 9, pp. 4854-4869.

[46] S. M. Bezrukov, I. Vodyanoy, "Noise-induced enhancement of signal trans-duction across voltage-dependent ion channels," *Nature*, 1995, vol. 378, no. 6555, pp. 362-364.

[47] A. R. Yaakub, D. J. Evans, "A fourth order Runge-Kutta $RK(4,4)$ method with error control," *International Journal of Computer Mathematics*, 1999, vol. 71, no. 3, pp. 383-411.

[48] F. Duan, D. Rousseau, F. Chapeaublondeau, "Residual aperiodic stochastic resonance in a bistable dynamic system transmitting a supra-threshold binary signal," *Physical Review E*, 2004, vol. 69, no. 1, pp. 383-391.

[49] J. Liu, Z. Li, L. Guan, et al., "A Novel Parameter-Tuned Stochastic Resonator for Binary PAM Signal Processing at Low SNR," *IEEE Communications Letters*, 2014, vol. 18, no. 3, pp. 427-430.

[50] J. T. Smith, J. T. Elkin, W. M. Reichert, "Directed cell migration on fibronectin gradients: effect of gradient slope," *Experimental cell research*, 2006, vol. 312, no. 13, pp. 2424-2432.

[51] Y. H. Lan, G. A. Papoian, "Stochastic resonant signaling in enzyme cascades," *Physical Review Letters*, 2007, vol. 98, no. 22, pp. 2117-2120.

[52] Y. K. Kwon, K. H. Cho, "Coherent coupling of feedback loops: a design principle of cell signaling networks," *Bioinformatics*, 2008, vol. 24, no. 17, pp. 1926-1932.

[53] S. H. Liu, Z. K. Wei, B. Li, W. S. Guo, C. L. Zhao, "Metric Combinations in non-coherent signal detection for molecular communication," *Nano Communication Networks*, 2019, doi: 10.1016/j.nancom.2019.02.001, pp. 1-10.